

Simulation of Steady-State Characteristics of Dye-Sensitized Solar Cells and the Interpretation of the Diffusion Length

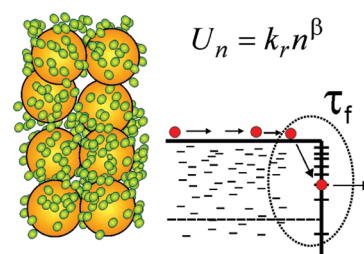
Juan Bisquert* and Iván Mora-Seró

Grup de Dispositius Fotovoltaics i Optoelectrònics, Departament de Física, Universitat Jaume I, 12071, Castelló, Spain

ABSTRACT Quantitative modeling of the photovoltaic response of the dye-sensitized solar cell (DSC) is an important subject for improving both the understanding of operation mechanisms and the device performance. A range of experimental techniques indicates that nonlinear recombination of the form $U_n = k_r n^\beta$, with $\beta \neq 1$, is a property of DSCs. We show that the diffusion length L_n defined from the probability of collection is independent of the macroscopic perturbation for $\beta \neq 1$ only for a small perturbation, and in this case, it coincides with the value $\lambda_n = (D_n \tau_n)^{1/2}$ that can be measured by impedance spectroscopy in homogeneous conditions. The increase of the diffusion length with the potential, usually observed experimentally, is attributed to the increase of the free carrier lifetime. We also discuss the modeling of real DSC devices under different conditions, and we conclude that the diffusion–recombination–generation equation based on $U_n = k_r n^\beta$ is a fundamental ingredient of the simulation tools.

SECTION Energy Conversion and Storage

Recombination in a DSC



With the continuing progress of dye-sensitized solar cells (DSC) and the appearance of different configurations and new components, it has become very important to establish the properties of the prepared DSC using a range of characterization methods, with a refined level of detail. Recently, some papers discussed the results on the diffusion length measured by small perturbation techniques, in comparison with a diffusion length measured from the collection efficiency.^{1–3} It is a very important task to correlate the results of different measurements in order to establish the significance of the parameters that govern the solar cell behavior. However, a problem in the interpretation of these results^{1–3} is that the diffusion length under steady-state conditions, and in the presence of nonlinear recombination, has not been generally defined. This is not a trivial question since for a recombination model that is not linear on carrier density, the lifetime depends heavily on the local concentration. However, the diffusion length cannot be defined on a point-to-point basis since it is a length that carriers travel before recombining. Here, we explore the meaning of the definition of the diffusion length in a nonlinear problem. We construct an analytical solution of this problem, and we discuss the interpretation of characteristic experimental results. We also discuss which are the main strategies for a useful characterization of the real DSC devices.

We present an introductory overview of the empirical evidence of recombination of DSCs. We highlight several important aspects of the DSC that have been consistently and independently observed in many laboratories, concerning the fill factor in current–potential curves, recombination resistance, and the dependence of open-circuit voltage on

illumination intensity. The starting point of our considerations is the well-known equation for diffusion, recombination, and generation at steady state

$$D_0 \frac{\partial^2 n}{\partial x^2} - U_n + G = 0 \quad (1)$$

In this equation, D_0 is the electron diffusion coefficient, U_n is the recombination rate per unit volume, and G is the generation rate. It is important to notice that we write the conservation eq 1 for the free electron concentration, n . In general, there are also trapping–detrapping effects that induce a density of electrons in localized states in the semiconductor bandgap, n_L , but these effects are described by time-dependent terms that do not contribute to eq 1.⁴ In a DSC, provided that the contact with the substrate is good and the electrolyte conductivity is high, we can relate the free electron density and the voltage V as

$$n = n_0 e^{qV/k_B T} \quad (2)$$

where k_B is Boltzmann's constant, T is the temperature, q is the elementary charge, and n_0 is an equilibrium concentration. Equation 1 provides the current–potential (I – V) characteristics of the solar cell provided that we take into account the thermal generation G_{thermal} .

The central question that we wish to treat in this Letter is the form of the recombination rate, U_n , and how this impacts

Received Date: November 21, 2009

Accepted Date: December 10, 2009

in all cases the modeling of real DSCs. A well-known model in photovoltaics uses the assumption

$$U_n = k_0 n \quad (3)$$

This is a linear model, amply used in silicon solar cells, for the minority carrier recombination. The linear model was proposed by Södergren et al.⁵ in an early stage in DSC research and has been profusely used in DSC modeling thereafter.

However, there is consistent and repeated evidence that the linear model cannot describe DSC characteristics quantitatively. We just mention two pieces of evidence. Important evidence about the recombination order arises from the recombination resistance measured in impedance spectroscopy (IS).^{6,7}

$$R_{\text{rec}} = \frac{1}{A} \left(\frac{\partial j_{\text{rec}}}{\partial V} \right)^{-1} \quad (4)$$

where j_{rec} is the recombination current and A is the cell area. For a layer of thickness L , we have $j_{\text{rec}} = qLU_n$, and we find that R_{rec} is related to a derivative of U_n as

$$R_{\text{rec}} = \frac{1}{qLA} \left(\frac{\partial U_n}{\partial V} \right)^{-1} \quad (5)$$

Now from eqs 2–4, it follows readily that $R_{\text{rec}} = R_0 \exp(-qV/k_B T)$ in the ideal (linear) model. However, this is far from true in the measurement of DSCs. The actual result follows the expression⁷

$$R_{\text{rec}} = R_0' \exp \left[-\beta \frac{qV}{k_B T} \right] \quad (6)$$

where the β parameter is typically in the range of 0.5–0.7.

By an integration of eq 4, one can easily see that the β parameter relates to the diode ideality factor as $m = 1/\beta$. Therefore, the appearance of an ideality factor $m > 1$ is another manifestation of nonlinear recombination in a DSC,⁸ see some examples in Figure 3b, below. However, the observation of $\beta < 1$ in IS measurements of resistance is perhaps even clearer evidence since the recombination resistance can be unambiguously separated from series and contact effects by the analysis in the frequency domain. In comparison, this is not always straightforward on current–potential curves. It should also be mentioned that Södergren et al.⁵ noticed that $m > 1$ was not consistent with their model;⁸ therefore, they tried to modify (ad hoc) the solution of the linear equation in the voltage dependence of the photocurrent. However, the measurements leading to eq 6 clearly show that the diode factor $m > 1$ arises from the recombination in the whole layer and not from any contact effects that may be incorporated as boundary conditions. To include a posteriori the nonideality factor is not a valid procedure since the continuity equation is nonlinear, and this has implications for the collection efficiency. Thus, any model based on eq 3 cannot consistently describe the experimental results.

A second, important piece of evidence is found in the measurement of the photovoltage dependence on illumination

intensity, Φ_0 . At open circuit, diffusion can be neglected, and eqs 1, 2, and 8 give the slope of the experimental curve as

$$\frac{dV_{\text{oc}}}{d \log \Phi_0} = \frac{k_B T}{2.30 \beta q} \quad (7)$$

which predicts a slope of 60 mV for linear recombination with $\beta = 1$. Again, the ideal model is far from the observations, which provide close to straight plots of V_{oc} versus $\log \Phi_0$ but with a slope which can reach 120 mV.^{8,9} Only in seldom cases is the 60 mV slope observed in a potential range.⁹

The results of measurements with different kinds of perturbation of the solar cell (electrical, as well as optical) are therefore consistent with a recombination rate of the type

$$U_n = k_r n^\beta \quad (8)$$

where k_r is a constant with units of $\text{cm}^{-3(1-\beta)} \text{s}^{-1}$. We should remark that although eq 8 is not strictly obeyed in all situations,¹⁰ it applies in many different types of DSCs over a significant voltage range, and therefore, it merits a detailed analysis as a first approach to nonlinear recombination.^{7,8,11}

One can also wonder what is the microscopic behavior of charge transfer that causes eq 8. It has been suggested that the power law behavior relates to the charge transfer via an exponential distribution of surface states, with parameter T_0 , which gives $\beta = 0.5 + T/T_0$.^{7,9,12} This approach has been amply discussed recently,^{10,13} but here, we are not concerned with the interpretation of eq 8. Rather, we take eq 8 as an empirically given reality and investigate the implications for steady-state modeling of the DSC.

Our goal is therefore to study the consequences of the equation

$$D_0 \frac{d^2 n}{dx^2} - k_r n^\beta + G = 0 \quad (9)$$

For clarity, we analyze only the case in which the generation rate G is homogeneous and much larger than thermal generation. In the absence of other sources of carriers, we have a constant density in all positions, which we term the background concentration

$$n_b = \left(\frac{G}{k_r} \right)^{1/\beta} \quad (10)$$

It is illustrative to recall the reference case of the linear recombination. Thus, for $\beta = 1$

$$\frac{d^2 n}{dx^2} - \frac{1}{L_1^2} (n - n_b) = 0 \quad (11)$$

The problem depends on a single length scale

$$L_1 = \left(\frac{D_0}{k_r} \right)^{1/2} \quad (12)$$

Now, we introduce the general definition of the diffusion length. To avoid any complications of boundaries, we consider infinite space $-\infty < x < \infty$. Diffusion and recombination of

generated and injected carriers is described by eq 9 with a constant G . We assume the injection of carriers by a point source at $x = 0$, and we define the diffusion length L_n as the average distance that injected carriers travel before disappearing.¹⁴ Since the equation is clearly symmetrical, we only need to consider the half space $0 \leq x < \infty$. Thus

$$L_n = \int_0^{+\infty} xf(x)dx \quad (13)$$

where the probability that a carrier is at position x is

$$f(x) = \frac{n(x) - n_b}{\int_0^{+\infty} [n(x) - n_b] dx} \quad (14)$$

Here, $n(x)$ is the solution of eq 9 with the following boundary conditions:

- (i) $n(0) - n_b$ is the concentration injected at $x = 0$ over the background, and
- (ii) $n = n_b$ at $x = +\infty$.

For the linear case in eq 11, the well-known solution is

$$n(x) = n_b + (n(0) - n_b)e^{-x/L_1} \quad (15)$$

If we insert eq 15 into eq 13, we obtain that eq 12 is indeed the diffusion length. In the case of $\beta = 1$, eq 9 is a linear equation, and all of the calculated responses, even for spatially dependent generation, are governed by a single constant length L_1 .⁵ This is because the response to an arbitrary stimulus can be calculated quite simply from the superposition of responses to point sources. However, this is far from true in a nonlinear problem; see section S1 of the Supporting Information.

We turn our attention to the analysis of the general case in eq 9. First of all, we observe that for $\beta \neq 1$, there is no constant with dimension of length. This is an early indication that a constant diffusion length such as L_1 is an exception that pertains only to the linear case. The physical reason for this is that in the nonlinear problem, the recombination rate depends strongly on the local concentration. We can reduce eq 9 to the convenient expression

$$\frac{d^2c}{dx^2} - \frac{1}{\lambda_0^2}c^\beta + g = 0 \quad (16)$$

Here, we have introduced a normalized concentration $c = n/n_b$ and generation

$$g = \frac{G}{D_0 n_b} = \frac{G^{1-1/\beta} k_r^{1/\beta}}{D_0} \quad (17)$$

and

$$\lambda_0 = \left(\frac{D_0 n_b^{1-\beta}}{k_r} \right)^{1/2} \quad (18)$$

is the length scale of the problem that now depends on n_b (note that λ_0 is not a diffusion length, which is given below).

In order to compute diffusion lengths, we need to solve eq 16 with the boundary conditions indicated above. Since we are only interested here in the case in which g is constant, we

can apply a procedure¹⁵ to obtain a first integral. From eq 16

$$\frac{1}{2} \left(\frac{dc}{dx} \right)^2 - \frac{1}{(\beta+1)\lambda_0^2} c^{\beta+1} + gc = K \quad (19)$$

where K is a constant of integration. By application of the boundary condition (ii), we can set $dc/dx = 0$ at $c = 1$. This fixes the constant K , and we get

$$\frac{1}{2} \left(\frac{dc}{dx} \right)^2 - \frac{1}{(\beta+1)\lambda_0^2} (c^{\beta+1} - 1) + g(c-1) = 0 \quad (20)$$

A second integration gives

$$x = -\frac{1}{\sqrt{2}} \int_{c(0)}^c \left[\frac{1}{(\beta+1)\lambda_0^2} (c^{\beta+1} - 1) - g(c-1) \right]^{-1/2} dc \quad (21)$$

Equation 21 can be computed numerically and inverted to give $c(x)$. The results are shown in Figure 1a for $\beta = 0.5$. It is observed that the concentration decays smoothly from $n(0)$ to the background value, n_b , which is marked in gray.

Before we discuss the results of $n(x)$ for this model, let us consider an important aspect of the problem that is related to the small perturbation measurement such as IS, time transients, and so forth. We notice in Figure 1a that when the injected concentration is $n(0) - n_b \ll n_b$, recombination will be basically fixed by the value of the background concentration at all points of space. Therefore, in eq 9, we can write $n(x) = n_b + n_1$, with $n_1 \ll n_b$. The terms in n_b cancel out by eq 10; see section S2 of the Supporting Information. The remaining equation for n_1 is

$$D_0 \frac{d^2 n_1}{dx^2} - \frac{1}{\tau_f} n_1 = 0 \quad (22)$$

Here, τ_f is the lifetime of free carriers, which has been defined elsewhere¹⁰ as

$$\tau_f = \left(\frac{\partial U_n}{\partial n} \right)^{-1} \quad (23)$$

and for eq 8, this gives

$$\tau_f = \frac{n_b^{1-\beta}}{\beta k_r} = \frac{n_0^{1-\beta}}{\beta k_r} \exp \left[\frac{q(1-\beta)V}{k_B T} \right] \quad (24)$$

We observe that eq 22 is linear just as eq 11. By reference to the linear case, in eq 22, we can introduce the small perturbation diffusion length

$$\lambda_n = \sqrt{D_0 \tau_f} \quad (25)$$

In the case $\beta = 1$, we obtain obviously $\lambda_n = L_1$, independent of background concentration, which is the standard definition of the diffusion length in terms of the small perturbation lifetime. However, in general

$$\lambda_n = \left(\frac{D_0 n_b^{1-\beta}}{\beta k_r} \right)^{1/2} = \frac{n_b^{-\beta/2}}{\beta^{1/2}} \lambda_0 \quad (26)$$

With respect to the measurements, it should be emphasized that D_0 and τ_f are usually not directly accessible. We can

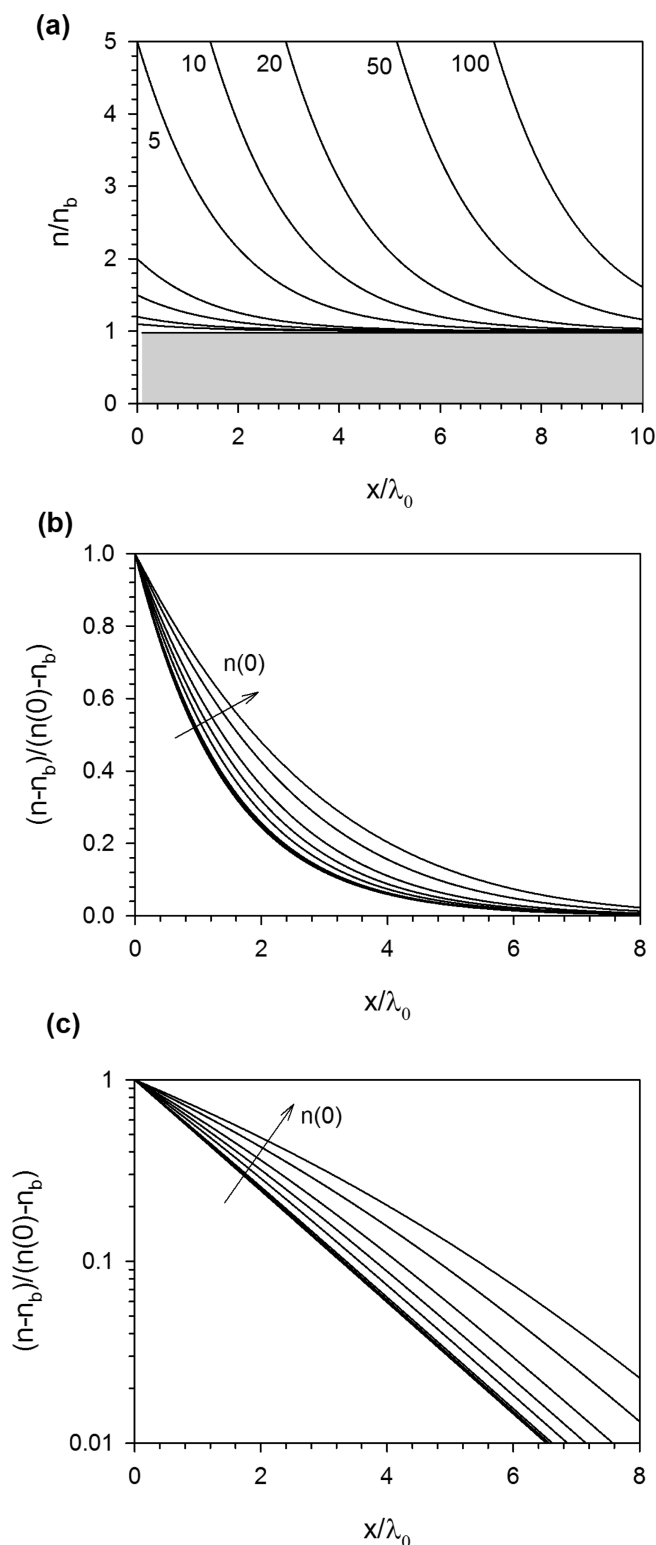


Figure 1. Representation of the decay of excess concentration injected at $x = 0$, for diffusion and nonlinear recombination with $\beta = 1/2$, in a background concentration. The different graphs show different normalization and scales of the same decays. Parameters $D_0 = k_r = G = 1$.

determine the small perturbation diffusion length from the quantities measured by small perturbation methods,⁴

namely, the chemical diffusion coefficient, D_n , and the lifetime, τ_n , as

$$\lambda_n = \sqrt{D_n \tau_n} \quad (27)$$

In a DSC, it is usually the case that there are trapping factors⁴ $\delta_L = \partial n / \partial n_L$ (see section S3 of the Supporting Information for further discussion), so that the measured diffusion coefficient and lifetime are

$$D_n = \delta_L D_0 \quad \tau_n = \tau_f / \delta_L \quad (28)$$

For example, for an exponential distribution of traps

$$\delta_L = A n^{1-\alpha} \quad (29)$$

where $\alpha = T/T_0$. If eq 28 is realized experimentally, the trapping factors disappear in the small perturbation diffusion length, and then, eq 27 gives eq 25 exactly.¹⁰

We have observed that for a small perturbation over a homogeneous background, the excess concentration is governed by the linear eq 22. We can thus infer that in such a situation, the calculation of the diffusion length in eq 13 will give

$$L_n = \lambda_n \quad (\text{for } n(0) - n_b \ll n_b) \quad (30)$$

The diffusion length is therefore well-defined for a small perturbation and measurable in a DSC, for example, by IS, even under nonlinear recombination, provided that the carrier distribution is homogeneous in the nanoporous layer. We also have the expression¹⁶

$$L_n = L \sqrt{\frac{R_{\text{rec}}}{R_{\text{tr}}}} \quad (31)$$

that relates the diffusion length to the recombination and transport resistances.

Usually, the measured lifetime in a DSC, τ_n , decreases with the bias voltage, but this is associated with a large trapping factor, eq 28. We remark that τ_f , the free carrier lifetime, increases with the bias voltage for $\beta < 1$ (the usual situation in a DSC); see eq 24. It follows from eqs 25 and 30 that L_n must increase with the bias voltage as well, and this is clearly observed in recent reports.^{2,3,17,18}

Let us discuss the general trends of the decay of injected carriers under the background concentration n_b that is shown in Figure 1. First, as already stated in eq 28, if $n(0) - n_b \ll n_b$, all decays have the same shape, which corresponds to the linear approximation in eq 22 and are represented with a thicker line in Figure 1 (because several decays give nearly the same response). This is observed in the normalized plot of Figure 1b, and the exponential shape is obvious in the log-linear plot of Figure 1c. The calculation of diffusion length by integration, eq 13, also confirms eq 30; see Figure 2. However, when $n(0) \approx 5n_b$ and larger, the decay profile departs from the linear model, and the diffusion length increases. Figure 1c shows that under large injection (with respect to background), the decays do not follow the exponential shape. If we attempt to determine the diffusion length using the linear approximation (exponential decay), we obtain an apparent diffusion length $L_{\text{exponential}}$ that is about twice L_n . If we determine the impedance response or other transient measurement under large injection, the free carrier

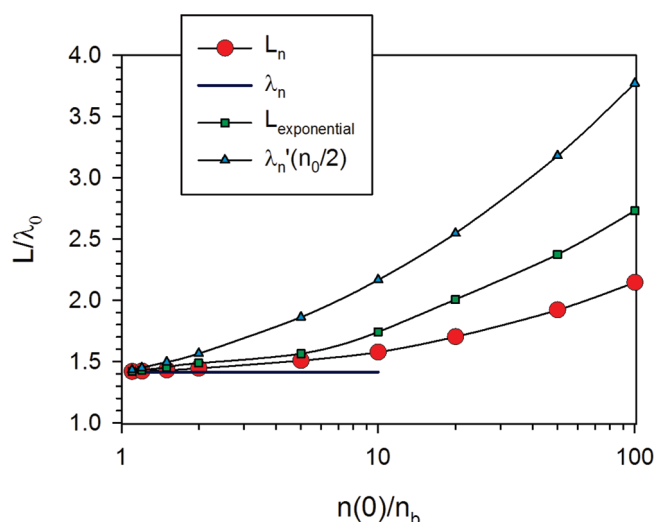


Figure 2. Representation of the diffusion length, L_n , for diffusion and nonlinear recombination with $\beta = 1/2$, over a background concentration, n_b , as a function of the injected density in a point source. The blue line is the small perturbation diffusion length, λ_n . The squares represent the approximate diffusion length obtained by fitting the decays to an exponential function. The triangles consist of calculating the small perturbation lifetime from the average concentration, $\lambda'_n(n_b + [n(0) - n_b]/2)$ (instead of the background concentration).

lifetime will correspond not with the carrier density n_b but with some homogeneous average concentration $\bar{n} \approx n_b + [n(0) - n_b]/2$. Furthermore, the correspondent diffusion length $\lambda'_n(n_0/2)$ calculated by eq 26 is even larger than the exponential approximation; see Figure 2.

This analysis provides the following conclusions. In the presence of nonlinear recombination, it is possible to associate a unique diffusion length to a set of external conditions only if the background concentration is uniform and the measuring perturbation is small. In this way, we obtain $L_n = \lambda_n = (D_n \tau_n)^{1/2}$, which is well-defined, independent of the amplitude of the perturbation, and this is shown experimentally in the agreement of $\lambda_n = (D_n \tau_n)^{1/2}$ measured by different methods.³ It is also possible to associate a diffusion length for a point source of large intensity since the background concentration becomes irrelevant. In this case, L_n is found by integration of the result of eq 21 and the definition in eq 13. In general, for other situations (e.g., with exponential generation profile or with the boundary condition of the solar cell, $[dn/dx]_{x=0} = 0$, etc.), the notion of a diffusion length should be confirmed with a full solution of the device model.

It is therefore convenient to conclude with a brief analysis the main strategies that one should adopt in modeling of DSC. To assist the discussion, we show in Figure 3a a set of current–potential (I/V) curves that are drawn using the well-known diode equation. All curves are physically feasible in the sense that current and efficiency are below the Shockley–Queisser (SQ) limit for the given band gap of the absorber. Curve A is a solar cell of low band gap, high current, and recombination governed by the linear model that gives the diode factor $m = 1$. This may be representative of silicon solar cells. Curve B, representing a DSC, produces a larger

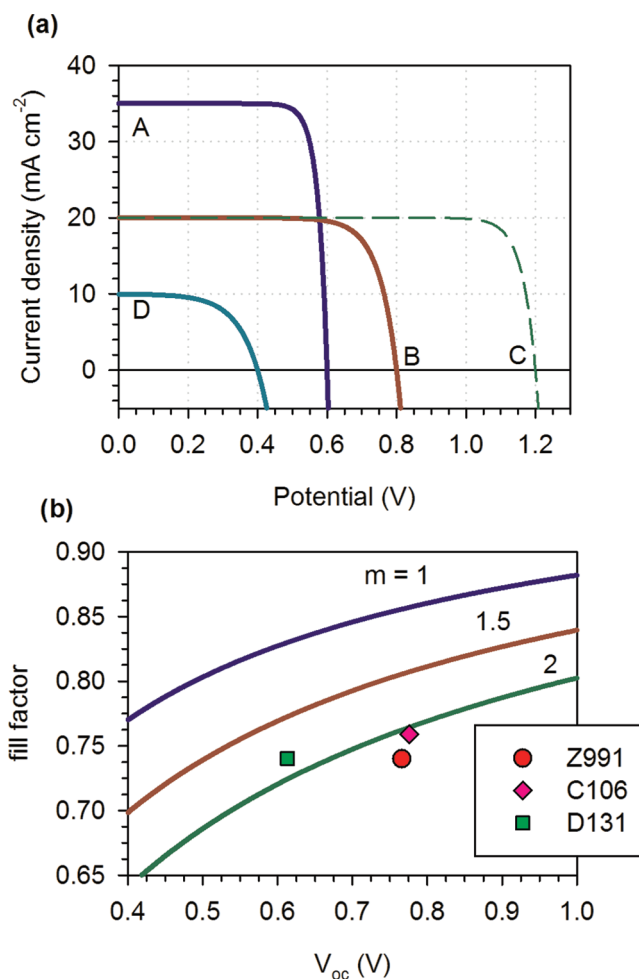


Figure 3. (a) Current density potential curves of solar cells at 1 sun (AM 1.5G) illumination with the following characteristics: (A) $m = 1$, FF = 0.82, $\eta = 17.3\%$; (B) $m = 2$, FF = 0.77, $\eta = 12.3\%$; (C) $m = 15$, FF = 0.86, $\eta = 20.3\%$; and (D) $\eta = 2.4\%$. (b) The fill factor of a Shockley diode as a function of the open-circuit potential, according to the value of the ideality factor, m . The points are values corresponding to characteristics of DSCs with dyes Z991 ($\eta = 12.2\%$),¹⁹ C106 ($\eta = 11.3\%$),¹⁷ and D131 ($\eta = 5.1\%$).²⁰

voltage but lower current than A, and the recombination with $\beta = 0.5$ gives a higher $m = 2$. This feature has an important impact on the reduction of power conversion efficiency since the fill factor decreases rapidly with increasing m ; see Figure 3b and section S4 of the Supporting Information. Under these conditions, the maximum photocurrent is reached, but this is not the case for the photovoltage. Even in the SQ limit, the maximal photovoltage does not reach the band gap (at AM 1.5G illumination) due to radiative recombination. In a real solar cell, V_{oc} is even lower due to (i) voltage losses in the device (contacts, alignment of energy levels, and so forth) or (ii) additional recombination pathways. In the current stressing work of pushing the DSC efficiency up, it is important to determine what is the best way to discriminate between these two limiting photovoltage factors. For example, for solar cells of type B, the given photocurrent could provide a much larger voltage, even allowing for some overvoltage between the absorber and the electron and

hole-transport materials. Thus, solar cell C could be reached by a DSC type, in principle. Therefore, a question arises about solar cell B, what is causing the limit of photovoltage? There are energetic limitations due to the specific electron and hole-transport materials used,²¹ but nonetheless, it is necessary to check if the recombination rate allows for such limits to be reached, that is, if the Fermi level of electrons in TiO₂ really gets right to the conduction band level.²² We observe in Figure 3b that real high efficiency DSCs provide fill factors around the value corresponding to $m = 2$. We assume that the influence of the series resistance in such cells must be very small.

For a detailed analysis of these features, it is important to obtain both the recombination resistance and the lifetime, even in the flat region of the *IV* curve and also close to V_{oc} ; see section S6 of the Supporting Information. These magnitudes are essential for the study of solar cell performance, while the diffusion length only can be defined as a global parameter in the linear case of eq 9, which is not obeyed by DSCs. More concretely, F. Fabregat-Santiago and co-workers showed¹¹ that R_{rec} is central for a proper reconstruction of the *IV* curve, and our discussion above indicates that the free carrier lifetime, τ_f , provides the fundamental information on recombination.¹⁰ Description of these experimental data, in the route toward higher voltages, requires eq 9 as the basic starting point.

Finally, one often finds in the literature the analysis of cells of low performance of the type D. For example, it has recently been observed that in some sets of metal-free organic dyes, the recombination increases strongly when the conjugation length is increased to shift the light absorption to the red part of the solar spectrum.^{23,24} In such cells, it is found, as in D, that the flat collection region is absent, indicating a decrease in the collection efficiency; see section S5 of the Supporting Information.²³ A detailed recombination model is necessary to describe such a system. It should be also mentioned that in addition to the electronic aspects described by eq 9, there may be considerable complexity of the transport of the hole-transport material, especially in viscous solvents or organic hole conductors, and also additional recombination pathways.²⁵ However, useful simulation tools should be consistent with the electronic properties of the DSCs that have been established by experience of many years in many different laboratories. This points out the need for more robust simulation programs that allow a proper interpretation of the data, with a combined and consistent analysis of impedance and steady-state data in combination with other useful methods. Some steps in this direction are taken recently by J. A. Anta and co-workers by adapting *IV* data to eq 9.²⁶ It is also important to develop a detailed description of the collection efficiency in a DSC starting with the nonlinear recombination model of eq 9 in order to clarify some experimental results that were reported recently.^{1–3}

In summary, nonlinear recombination becomes manifest in measurements of DSCs, especially in the recombination resistance dependence on voltage and in the dependence of the photovoltage on illumination intensity. We have suggested that a starting model to describe such properties is based on the free carrier lifetime and recombination resistance dependence on carrier density and on the compensation of trapping

factors. These two properties imply the increase of the diffusion length with voltage, as observed experimentally, but a more systematic study of the validity of the two assumptions should be carefully investigated. Modeling of the steady-state behavior of a DSC should start with the diffusion–recombination–generation equation, in which recombination order β is consistent with that obtained from the recombination resistance. In some situations, especially in very low performance solar cells, the collection efficiency becomes an issue and should be further investigated consistently with the generally valid simulation approach.

SUPPORTING INFORMATION AVAILABLE Definition of the diffusion length, the conservation equation, trapping factors, diode quality factors, theoretical *IV* curves, and the diffusion length in terms of resistances. This material is available free of charge via the Internet at <http://pubs.acs.org>.

AUTHOR INFORMATION

Corresponding Author:

*To whom correspondence should be addressed. Email: bisquert@fca.uji.es.

ACKNOWLEDGMENT Our views on the fundamental description of DSCs have been aided by discussions with many colleagues, and in particular, we wish to acknowledge conversations with Francisco Fabregat Santiago, Michael Grätzel, Jane Halme, Laurie Peter, and Difei Zhou. The work was supported by Ministerio de Ciencia e Innovación of Spain under Projects Consolider HOPE CSD2007-00007 and MAT2007-62982 and by Generalitat Valenciana project PROMETEO/2009/058.

REFERENCES

- (1) Halme, J.; Boschloo, G.; Hagfeldt, A.; Lund, P. Spectral Characteristics of Light Harvesting, Electron Injection, and Steady-State Charge Collection in Pressed TiO₂ Dye Solar Cells. *J. Phys. Chem. C* **2008**, *112*, 5623–5637.
- (2) Barnes, P. R. F.; Anderson, A. Y.; Koops, S.; Durrant, J. R.; O'Regan, B. Electron Injection Efficiency and Diffusion Length in Dye-Sensitized Solar Cells Derived from Incident Photon Conversion Efficiency Measurements. *J. Phys. Chem. C* **2009**, *113*, 1126–1136.
- (3) Wang, H.; Peter, L. M. A Comparison of Different Methods To Determine the Electron Diffusion Length in Dye-Sensitized Solar Cells. *J. Phys. Chem. C* **2009**, *113*, 18125–18133.
- (4) Bisquert, J.; Vikhrenko, V. S. Interpretation of the Time Constants Measured by Kinetic Techniques in Nanostructured Semiconductor Electrodes and Dye-Sensitized Solar Cells. *J. Phys. Chem. B* **2004**, *108*, 2313–2322.
- (5) Södergren, S.; Hagfeldt, A.; Olsson, J.; Lindquist, S. E. Theoretical Models for the Action Spectrum and the Current–Voltage Characteristics of Microporous Semiconductor Films in Photoelectrochemical Cells. *J. Phys. Chem.* **1994**, *98*, 5552–5556.
- (6) Fabregat-Santiago, F.; Bisquert, J.; Garcia-Belmonte, G.; Boschloo, G.; Hagfeldt, A. Impedance Spectroscopy Study of the Influence of Electrolyte Conditions in Parameters of Transport and Recombination in Dye-Sensitized Solar Cells. *Sol. Energy Mater. Sol. Cells* **2005**, *87*, 117–131.

- (7) Wang, Q.; Ito, S.; Grätzel, M.; Fabregat-Santiago, F.; Mora-Seró, I.; Bisquert, J.; Bessho, T.; Imai, H. Characteristics of High Efficiency Dye-Sensitized Solar Cells. *J. Phys. Chem. B* **2006**, *110*, 19406–19411.
- (8) Huang, S. Y.; Schilchthörl, G.; Nozik, A. J.; Grätzel, M.; Frank, A. J. Charge Recombination in Dye-Sensitized Nanocrystalline TiO₂ Solar Cells. *J. Phys. Chem. B* **1997**, *101*, 2576–2582.
- (9) Salvador, P.; González-Hidalgo, M.; Zaban, A.; Bisquert, J. Illumination Intensity Dependence of the Photovoltage in Nanostructured TiO₂ Dye-Sensitized Solar Cells. *J. Phys. Chem. B* **2005**, *109*, 15915–15926.
- (10) Bisquert, J.; Fabregat-Santiago, F.; Mora-Seró, I.; Garcia-Belmonte, G.; Giménez, S. Electron Lifetime in Dye-Sensitized Solar Cells: Theory and Interpretation of Measurements. *J. Phys. Chem. C* **2009**, *113*, 17278–17290.
- (11) Fabregat-Santiago, F.; Bisquert, J.; Palomares, E.; Otero, L.; Kuang, D.; Zakeeruddin, S. M.; Grätzel, M. Correlation between Photovoltaic Performance and Impedance Spectroscopy of Dye-Sensitized Solar Cells Based on Ionic Liquids. *J. Phys. Chem. C* **2007**, *111*, 6550–6560.
- (12) Bisquert, J.; Zaban, A.; Salvador, P. Analysis of the Mechanism of Electron Recombination in Nanoporous TiO₂ Dye-Sensitized Solar Cells. Nonequilibrium Steady State Statistics and Transfer Rate of Electrons in Surface States. *J. Phys. Chem. B* **2002**, *106*, 8774–8782.
- (13) He, C.; Zheng, Z.; Tang, H.; Zhao, L.; Lu, F. Electrochemical Impedance Spectroscopy Characterization of Electron Transport and Recombination in ZnO Nanorod Dye-Sensitized Solar Cells. *J. Phys. Chem. C* **2009**, *113*, 10322–10325.
- (14) Amaldi, E.; Fermi, E. on the Absorption and the Diffusion of Slow Neutrons. *Phys. Rev.* **1936**, *50*, 899–928.
- (15) Magyari, E. Exact Analytical Solution of a Nonlinear Reaction-Diffusion Model in Porous Catalysts. *Chem. Eng. J.* **2008**, *143*, 167–171.
- (16) Bisquert, J. Theory of the Impedance of Electron Diffusion and Recombination in a Thin Layer. *J. Phys. Chem. B* **2002**, *106*, 325–333.
- (17) Cao, Y.; Bai, Y.; Yu, Q.; Cheng, Y.; Liu, S.; Shui, D.; Gao, F.; Wang, P. Dye-Sensitized Solar Cells with a High Absorptivity Ruthenium Sensitizer Featuring a 2-(Hexylthio)thiophene Conjugated Bipyridine. *J. Phys. Chem. C* **2009**, *113*, 6290–6297.
- (18) Fabregat-Santiago, F.; Bisquert, J.; Cevey, L.; Chen, P.; Wang, M.; Zakeeruddin, S. M.; Grätzel, M. Electron Transport and Recombination in Solid State Dye Solar Cell with spiro-OMeTAD as Hole Conductor. *J. Am. Chem. Soc.* **2009**, *131*, 558–562.
- (19) Grätzel, M. Optimizing Photon Harvesting and Carrier Collection in Mesoscopic Solar Energy Conversion Systems. Presentation at MRS Fall Meeting, Boston, MA, 2009.
- (20) Ogura, R. Y.; Nakane, S.; Morooka, M.; Orihashi, M.; Suzuki, Y.; Noda, K. High-Performance Dye-Sensitized Solar Cell with a Multiple Dye System. *Appl. Phys. Lett.* **2009**, *94*, 073508.
- (21) Bisquert, J.; Cahen, D.; Rühle, S.; Hodes, G.; Zaban, A. Physical Chemical Principles of Photovoltaic Conversion with Nanoparticulate, Mesoporous Dye-Sensitized Solar Cells. *J. Phys. Chem. B* **2004**, *108*, 8106–8118.
- (22) Cahen, D.; Hodes, G.; Grätzel, M.; Guillemoles, J. F.; Riess, I. Nature of Photovoltaic Action in Dye-Sensitized Solar Cells. *J. Phys. Chem. B* **2000**, *104*, 2053–2059.
- (23) Barea, E. M.; Caballero, R.; Fabregat-Santiago, F.; de la Cruz, P.; Langa, F.; Bisquert, J. Bandgap Modulation in Efficient *n*-Thiophene Absorbers for Dye Solar Cell Sensitization. *ChemPhysChem* 2009, doi: 10.1002/cphc.200900605.
- (24) Marinado, T.; Nonomura, K.; Nissfolk, J.; Karlsson, M. K.; Hagberg, D. P.; Sun, L.; Mori, S.; Hagfeldt, A. How the Nature of Triphenylamine-Polyene Dyes in Dye-Sensitized Solar Cells Affects the Open-Circuit Voltage and Electron Lifetimes. *Langmuir* 2009, doi: 10.1021/la902897z.
- (25) Hamman, T. W.; Jensen, R. A.; Martinson, A. B. F.; Ryswykac, H. V.; Hupp, J. T. Advancing beyond Current Generation Dye-Sensitized Solar Cells. *Energy Environ. Sci.* **2008**, *1*, 66–78.
- (26) Villanueva-Cab, J.; Oskam, G.; Anta, J. A. A Simple Numerical Model for the Charge Transport and Recombination Properties of Dye-Sensitized Solar Cells: A Comparison of Transport-Limited and Transfer-Limited Recombination. *Sol. Energy Mater. Sol. Cells* **2010**, *94*, 45–50.

Supporting information

DOI: 10.1021/jz900297b | J. Phys. Chem. Lett. 2010, 1, 450–456

Simulation of steady-state characteristics of dye-sensitized solar cells and the interpretation of the diffusion length

Juan Bisquert* and Iván Mora-Seró

Grup de Dispositius Fotovoltàics i Optoelectrònics, Departament de Física, Universitat Jaume I, 12071, Castelló, Spain

S1.- Consistency of the definition of the diffusion length

Consider diffusion-recombination and generation for a constant free carrier lifetime (linear recombination)

$$D_0 \frac{d^2 n(x)}{dx^2} - \frac{1}{\tau_0} n(x) + G(x) = 0 \quad (\text{S1})$$

We solve the equation for an impulse that generates n_a at $x = 0$.

$$n(x) = n_a e^{-x/L_n} \text{ for } x \geq 0 .$$

$$n(x) = n_a e^{x/L_n} \text{ for } x \leq 0 . \quad (\text{S2})$$

where $L_n = \sqrt{D_0 \tau_0}$.

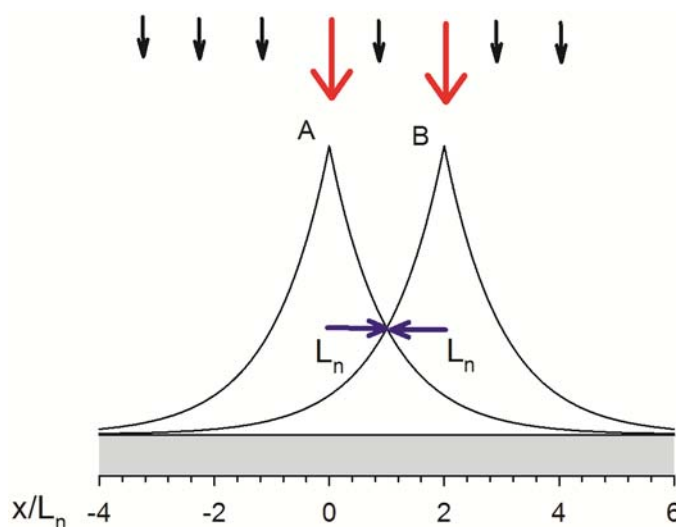


Fig. S1.1. Diffusion with linear recombination. The black lines are the distribution of carriers for isolated impulses. The blue arrow is the diffusion length from the point of injection.

If we consider several impulses, see Fig. S1.1, the resulting $n(x)$ can be simply obtained by addition of the solution to the individual source. The excess diffusing carriers of separate impulses do not interfere with each other. As an example in Fig. S1.1 we combine a constant generation at all points and two point sources. The diffusion length, i.e., the distance that carriers travel from point A, maintains the meaning for an arbitrary generation profile around the original source A.

For the non-linear equation

$$D_0 \frac{d^2 n}{dx^2} - k_r n^\beta + G(x) = 0 \quad (9)$$

the situation is quite different. The solution for two impulses is not the addition of the responses for the individual impulse. For example if the free carrier lifetime increases with the concentration, in Fig. S1.2 the flux to the right from source A will be enhanced by the presence of source B. The distance travelled from A depends on the particular situation along the way and cannot be defined as a general parameter.

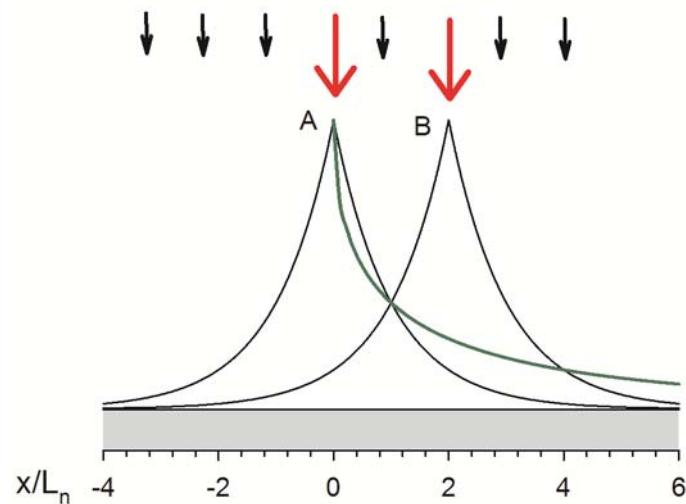


Fig. S1.2: Diffusion with nonlinear recombination. The black lines are the distribution of carriers for isolated impulses. The green line suggests the diffusion of

carriers generated at source A in the presence of source B.

S2.- Linealization of the conservation equation

We start from the following equation.

$$D_0 \frac{d^2 n(x)}{dx^2} - k_r n(x)^\beta + G(x) = 0 \quad (9)$$

Given a generation profile $G_{ss}(x)$ and boundary conditions, Eq. (9) has some solution that we denote $n_{ss}(x)$.

We apply some small perturbation (for example a slight change of the potential at the boundary). The new solution will be $n_{ss}(x) + n_1(x)$, where $n_1 \ll n_{ss}$. Eq. (9) is generally valid, therefore

$$D_0 \frac{d^2 (n_{ss} + n_1)}{dx^2} - k_r (n_{ss} + n_1)^\beta + G(x) = 0 \quad (S2.1)$$

The term in k_r can be simplified by expansion to first order

$$-k_r (n_{ss} + n_1)^\beta = -k_r n_{ss}^\beta \left(1 + \frac{n_1}{n_{ss}}\right)^\beta = -k_r n_{ss}^\beta \left(1 + \beta \frac{n_1}{n_{ss}}\right) \quad (S2.2)$$

Returning to (S2.1) we can separate two equations. The first is eq (9) for n_{ss} . The second is the linear equation

$$D_0 \frac{d^2 n_1(x)}{dx^2} - k_r \beta n_{ss}^{\beta-1}(x) n_1(x) = 0 \quad (S2.3)$$

If n_{ss} is homogeneous (uniform G) then $n_{ss} = n_b$. This is the case described in eq (22) of the text.

If n_{ss} is position-dependent then we must solve the eq (9) for $n_{ss}(x)$ and this enters the equation (S2.3) for $n_1(x)$. For example the impedance problem can be formulated in terms of the equations

$$J_1(x) = -D_0 \frac{dn_1(x)}{dx} \quad (S2.4)$$

$$\frac{\partial n_1(x)}{\partial t} = -\frac{\partial J_1(x)}{\partial x} - k_r \beta n_{ss}^{\beta-1}(x) n_1(x) \quad (S2.5)$$

S3.- Trapping factors

In the presence of traps, the time-dependent conservation equation for free carriers,

n_c , contains an additional term, due to the net capture by traps, which increase the concentration of localized electrons n_L .

$$\frac{\partial n_c}{\partial t} = -\frac{\partial J}{\partial x} - k_r n_c^\beta - \frac{\partial n_L}{\partial t} \quad (\text{S3.1})$$

Eq (S3.1) may be completed by a kinetic equation for the traps that defines the variation $\partial n_L / \partial t$. However, if the trapping kinetics is fast we may assume that the traps follow the equilibrium relation with the free carriers

$$\frac{\partial n_L}{\partial t} = \frac{\partial n_L}{\partial n_c} \frac{\partial n_c}{\partial t} \quad (\text{S3.2})$$

Therefore eq (S3.1) is written

$$\left(1 + \frac{\partial n_L}{\partial n_c}\right) \frac{\partial n_c}{\partial t} = -\frac{\partial J}{\partial x} - k_r n_c^\beta \quad (\text{S3.3})$$

We introduce the trapping factor

$$\delta_L = \left(1 + \frac{\partial n_L}{\partial n_c}\right) \approx \frac{\partial n_L}{\partial n_c} \quad (\text{S3.4})$$

Equation (S3.3) takes the form

$$\frac{\partial n_c}{\partial t} = \frac{D_0}{\delta_L} \frac{\partial^2 n_c}{\partial x^2} - \frac{k_r}{\delta_L} n_c^\beta \quad (\text{S3.5})$$

For a small perturbation,

$$\frac{\partial n_{c1}}{\partial t} = \frac{D_0}{\delta_L} \frac{\partial^2 n_{c1}}{\partial x^2} - \frac{1}{\delta_L \tau_f} n_{c1} \quad (\text{S3.6})$$

For a time dependent small perturbation, we can treat the system in terms of the free carriers but the measured diffusion coefficient and lifetime are

$$D_n = D_0 / \delta_L \quad (\text{S3.7})$$

$$\tau_n = \delta_L \tau_f \quad (\text{S3.8})$$

For a steady state situation, the trapping factors do not contribute and the conservation equation is

$$D_0 \frac{\partial^2 n_c}{\partial x^2} - k_r n_c^\beta = 0 \quad (\text{S3.9})$$

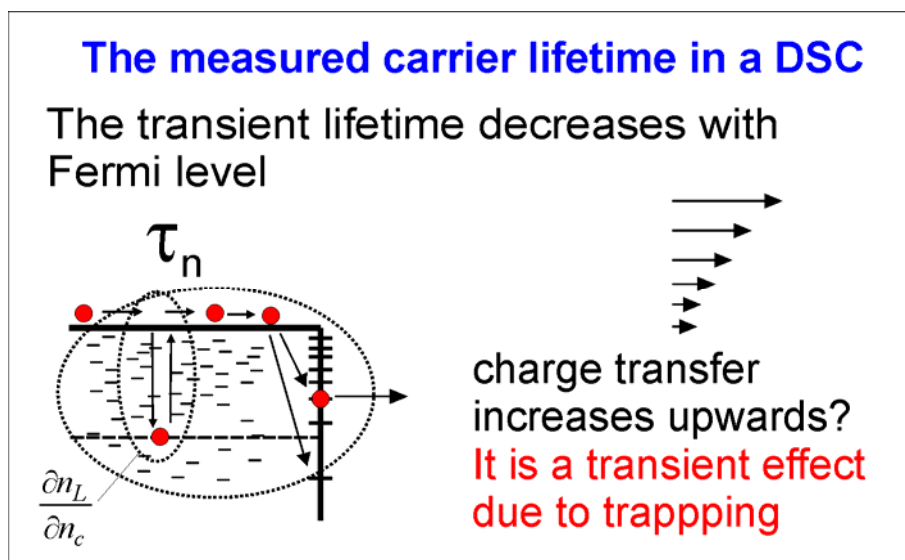
The essence of the quasistatic approximation, is to describe the kinetic factors for trapping and detrapping in terms of occupation of free and localized states. This is

possible because the kinetic constants for forward and reverse processes are linked by detailed balance to the occupation of the states from which the transitions occur, and this is succinctly expressed in eq (S3.2). The quasistatic approximation was introduced to account for the properties of measured time constants in DSC in Ref. ¹. For a complete explanation of this approach see Refs ¹⁻³

The compensation of the trapping factors¹ in the small perturbation diffusion coefficient is not complete if the free carrier lifetime shows some dependence with the potential, as implied by eq (24)

$$\tau_f = \frac{n_0^{1-\beta}}{\beta k_r} \exp\left[\frac{q(1-\beta)V}{k_B T}\right] \quad (24)$$

Therefore, the lifetime, τ_n , that is measured by the decay of the Fermi level, decreases with the potential, but this can be attributed mostly to the trapping factor. While the relevant lifetime for steady state conditions is the free carrier lifetime, τ_f , which increases with the bias as indicated in eq. (24). This is explained in the following diagrams, Fig. S3.1. The characteristic variation of parameters with voltage in a DSc is described in Fig. S3.2, and the variation of parameters with the temperature is illustrated in Fig. S3.3.



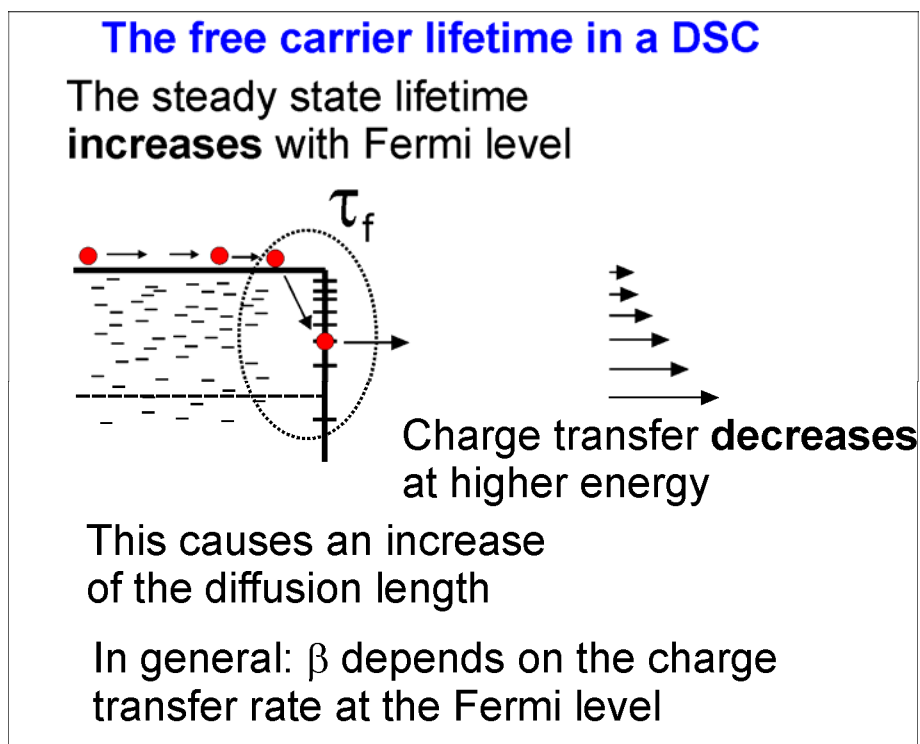


Fig. S3.1. Schematic view of the electron lifetime measured by small perturbation, τ_n (top panel) and the free carrier lifetime, τ_f (bottom panel), and the implications for the diffusion length in the case that recombination is determined by a constant $\beta < 1$. The set of arrows indicates the change of charge transfer rates.

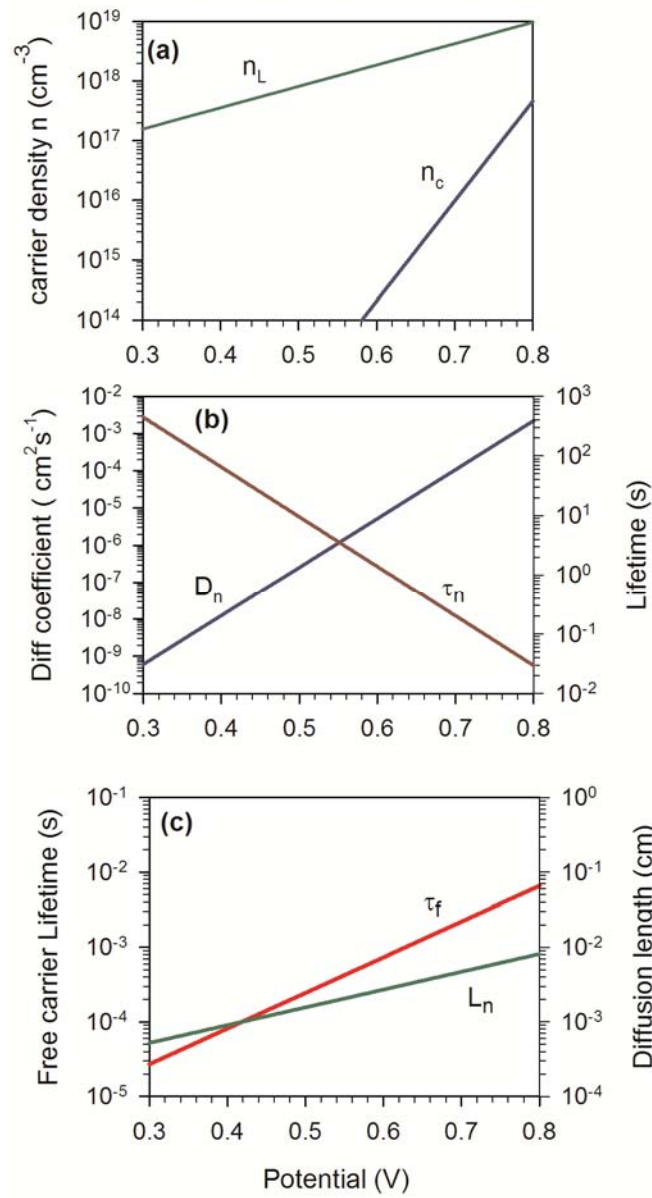


Fig. S3.2. (a) Representation of the free and localized carrier density, as a function of potential (Fermi level position), for an exponential distribution of localized states ($T = 300 \text{ K}$, $T_0 = 1400 \text{ K}$, $\beta = 0.5 + T/T_0 = 0.71$). (b) Electron lifetime, τ_n , and the diffusion coefficient, D_n , measured by small perturbation. (c) The free carrier lifetime, τ_f , and diffusion length $L_n = \sqrt{D_n \tau_n} = \sqrt{D_0 \tau_f}$.

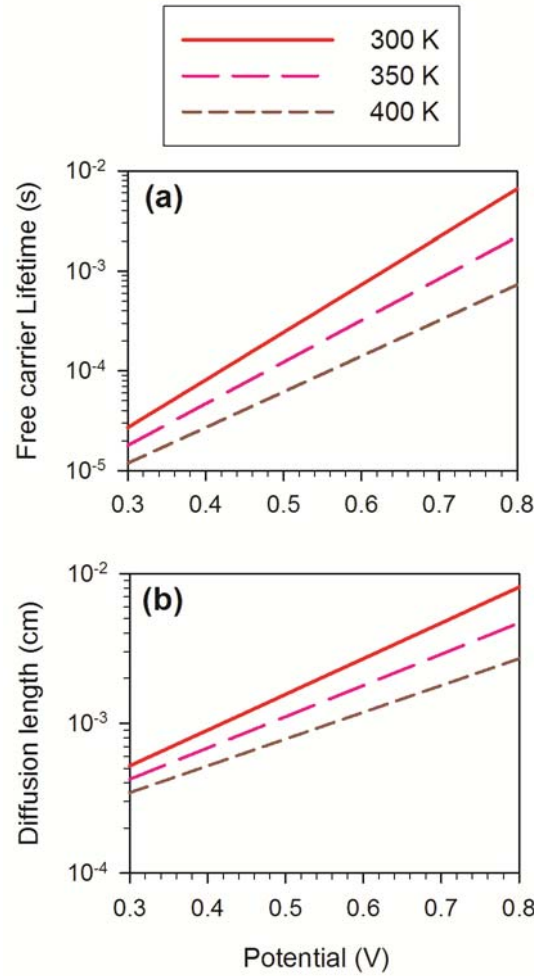


Fig. S3.3. (a) Representation the free carrier lifetime, τ_f , and diffusion length $L_n = \sqrt{D_n \tau_n} = \sqrt{D_0 \tau_f}$ as a function of potential (Fermi level position), for an exponential distribution of localized states ($T_0 = 1400$ K, $\beta = 0.5 + T/T_0$) at different temperatures. See experimental data in Refs. ^{3,4}.

S4.- Diode quality factors

The fill factor (FF) of a Shockley diode is found readily, by solving the potential that gives the maximum power of the IV characteristics. The result is only a function of the open-circuit voltage, V_{oc} . $FF(V_{oc})$ is found with excellent approximation by the analytically closed expression given by M. Green in 1980 [*Solar Cells: Operating Principles, Technology and Systems Applications*]

$$FF(V_{oc}) = \frac{V_{oc}/V_r - \ln(V_{oc}/V_r + 0.72)}{V_{oc}/V_r + 1} \quad (\text{S4.1})$$

where $V_r = qV_{oc}/(mk_B T)$. Fill factors are shown in Fig. 3(b) as a function of V_{oc} .

It should be emphasized that eq. (S4.1) is obtained from a model in which the probability of collection is independent of the potential. Since a DSC current-potential curve must be based on a more general equation such as (9), the equation (S4.1) for the FF as a function of V_{oc} must be considered a first approximation.

S5.- IV curves for linear recombination

In order to clarify comments in the main text referred to Fig. 3, we have simulated several IV curves with different parameters. To obtain the IV curves we have integrated the linear equation (S5.1)^{5,6} for reason of simplicity:

$$D_0 \frac{\partial^2 n(x)}{\partial x^2} - \frac{n(x) - n_0}{\tau_0} + \alpha_a \Phi \exp(-\alpha x) = 0 \quad (\text{S5.1})$$

We have considered a non-homogeneous, exponential absorption, where α_a is the absorption coefficient and Φ in the incident light intensity. The boundary conditions employed considering substrate side illumination are:

- (i) $n(0)$ relates to the bias voltage V as determined by eq. (2).
- (ii) $J(x = L) = 0$ where L is the length of the sample.

Fig. S5.1a shows the IV curves considering a constant diffusion coefficient and lifetime, τ_0 . Fig. S5.1a plots the IV curves using different diffusion length (unambiguously defined in the linear case): $10L$, L and $0.1L$. The collection efficiency moves to significantly lower than 100% when the diffusion length is of the same magnitude or lower than the sample length as it is commonly know. But it is important to point out that in the three cases IV curves follow the same pattern: with a flat part at lower voltages and an exponential decrease at the higher ones due to recombination. In the case of a DSC the diffusion length is not a good parameter when the recombination is non-linear, as it has been pointed out in the main text. The question is what is the good magnitude to differentiate between good and bad performing cells, taking into account that both presents the same IV pattern.

We want to show that recombination resistance is a good magnitude to clarify this point. In the case of linear recombination defined in (S5.1), with the boundary conditions commented, recombination resistance can be calculated as:

$$R_{rec} = \left(\frac{\partial J_{rec}(x=0)}{\partial V} \right) = \left(\frac{\partial J(x=0)}{\partial V} \right) = \frac{kT\tau}{L_n q^2} \frac{\cosh\left(\frac{L}{L_n}\right)}{\sinh\left(\frac{L}{L_n}\right)} \frac{1}{n} \quad (\text{S5.2})$$

Note that $J = J_{rec} - J_{gen}$ and the generation current, J_{gen} , is constant and dependent of the light intensity. J_{rec} is the recombination current. Fig. S5.1b shows the recombination resistance, R_{rec} , for the three cells simulated in Fig. S5.1a. It should be remarked that in the flat part of the IV curve, recombination resistance R_{rec} shows an exponential variation and informs us about recombination rate in all conditions of the solar cell. This is because R_{rec} is a derivative of the current that removes the voltage-independent contributions, eq (4) and (S5.2). Therefore R_{rec} gives us a key magnitude to discriminate between these cells, and can be unambiguously defined, even in the case of non-linear recombination, as it has been shown in the main text. It can be easily measured by IS.

On the other hand a cell, as B in Fig. 3, can have a 100% of collection efficiency but does not reach its maximum potential photovoltage due to recombination, see Fig. S5.1c. Again, R_{rec} allow us to identify this effect, see Fig. 5.1d. An increase of R_{rec} moves the point where recombination reduces the current to higher voltage, and R_{rec} increases. Obviously the photocurrent is not affected since it has in all cases the maximal possible value, determined by the convolution of the absorbance of the absorber material and the spectral flux of photons.

The present study should be completed with the correspondent analysis based on non-linear recombination, eq (9). This will be presented in a forthcoming publication.

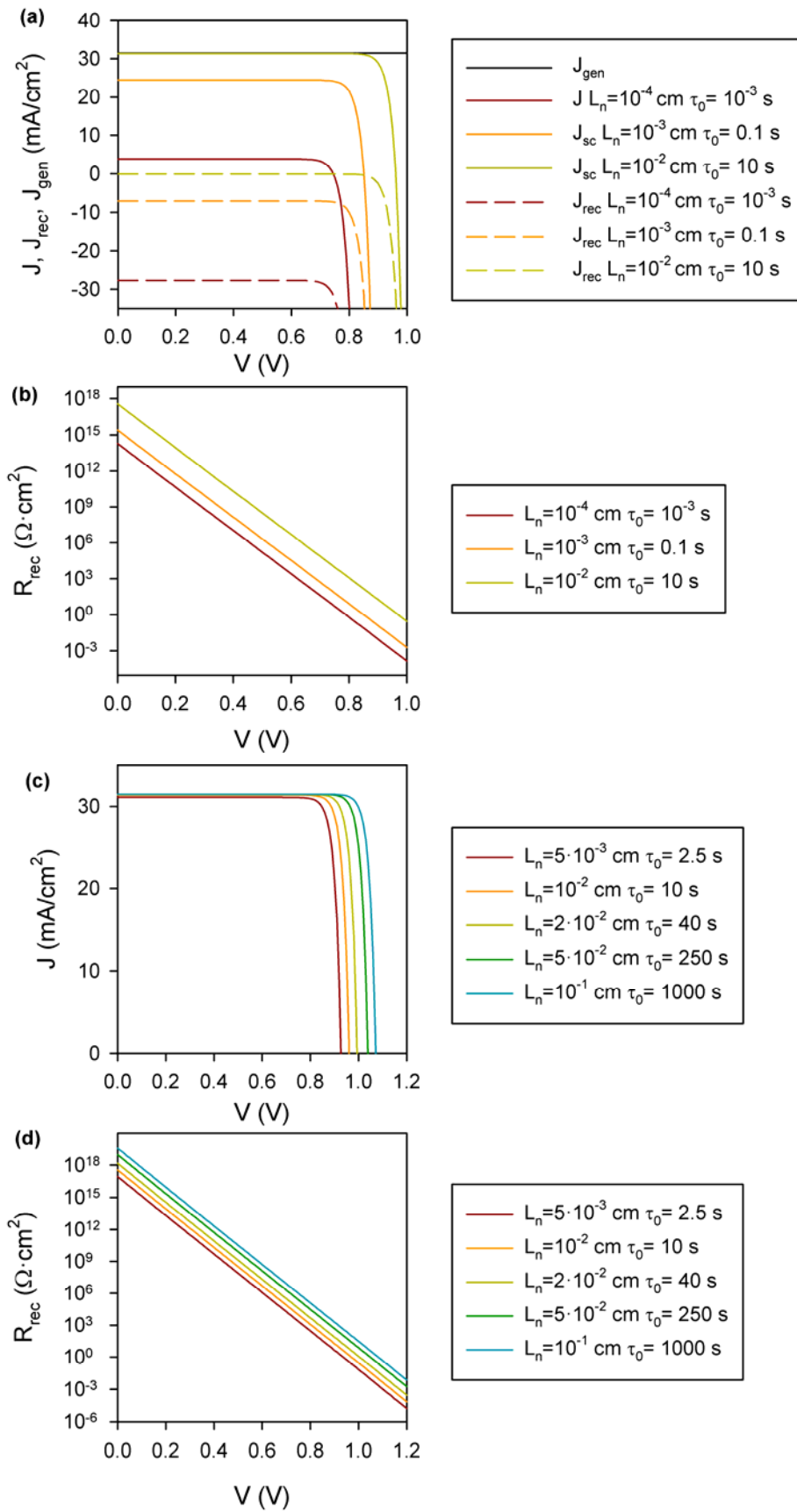


Fig. S5: a & c) IV curves from the integration of equation (S5.1). **b&d)** Recombination resistances. $D_0 = 10^{-5} \text{ cm}^2 \cdot \text{s}^{-1}$, $L = 10^{-3} \text{ cm}$, $\Phi = 5 \cdot 10^{17} \text{ cm}^{-2} \cdot \text{s}^{-1}$, $T = 300 \text{ K}$, $\alpha = 500 \text{ cm}^{-1}$.

S6.- Diffusion length in terms of measured resistances

An evaluation of the collection efficiency requires to compare the rate of transport and the rate of recombination in the active layer of the solar cell. The expression⁷

$$L_n = \lambda_n = L \sqrt{\frac{R_{rec}}{R_{tr}}} \quad (31)$$

relates the diffusion length to the recombination and transport resistances.

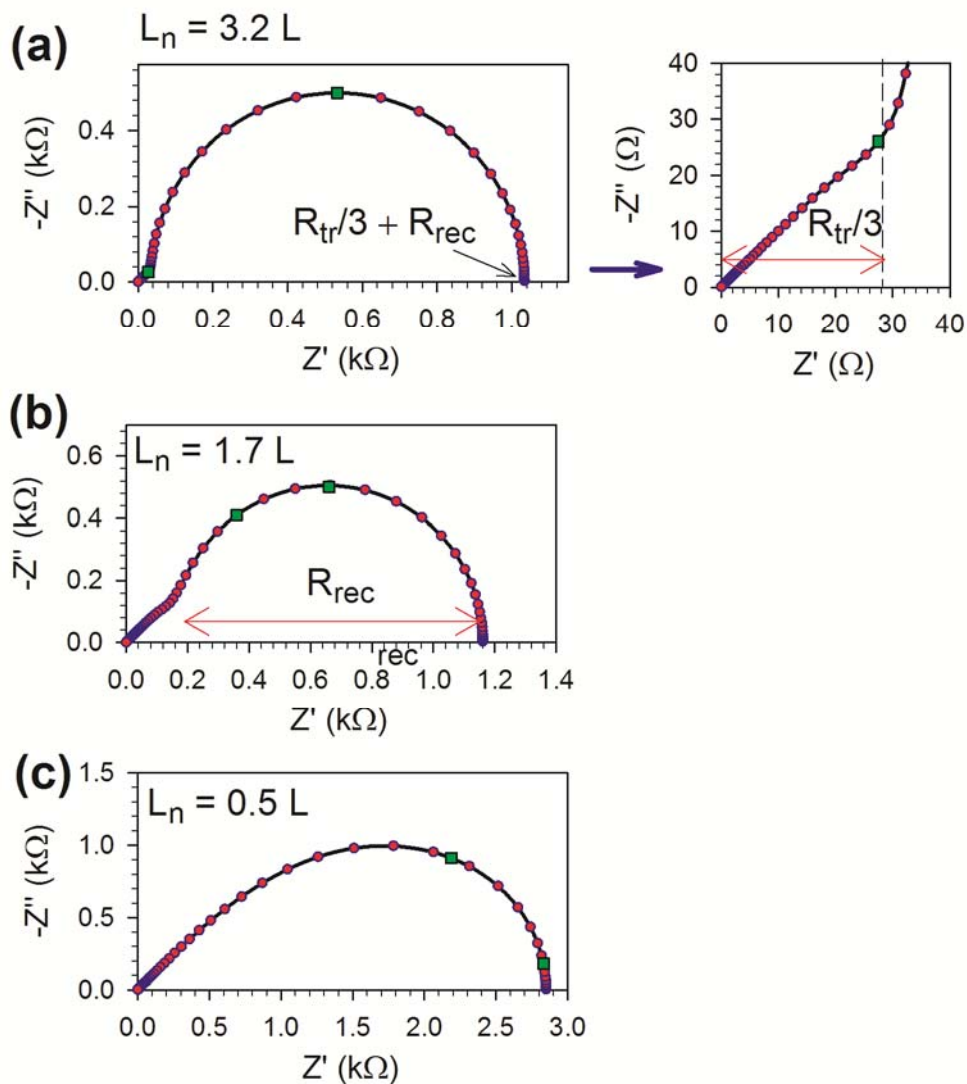


Fig. S6: The impedance spectra in diffusion-recombination model, at decreasing ratios R_{rec}/R_{tr} .

It was shown⁷ that the ratio R_{rec} / R_{tr} provides different types of spectra, as shown in Fig. S6. If $R_{rec} \gg R_{tr}$ the recombination resistance forms a large arc at low frequency, and the transport resistance forms a small Warburg feature at high frequency, Fig. S6a. This type of spectrum allows to immediately recognize a DSC with a large collection efficiency.⁸ In contrast, when recombination flux is large and we have the situation $R_{rec} < R_{tr}$ we obtain the Gerisher impedance which indicates that not all carriers can be extracted from the sample, Fig. S6c. In the Gerisher impedance R_{tr} and R_{rec} cannot be distinguished by inspection and a fit of the spectra is necessary to determine these parameters.

The impedance model was solved for homogeneous conditions of carrier distribution,⁷ and for situations in which the carriers are not homogeneous, a numerical solution based on eqs (S2.4) and (S2.5) should be attempted.⁹

It interesting to observe that in Fig. S6a (high collection efficiency) capacitances (or time constants) are not necessary to appreciate the collection efficiency, which is given by competition of transport and recombination *fluxes* that are directly evaluated by the correspondent resistances. The capacitive behaviour is however important to discriminate the different resistive components from the total resistance. The power of IS is to provide both resistances and the discrimination method in a single spectroscopy.

In the case of low collection efficiency, Fig. S6c, it is important to remark that the two processes of transport and recombination are closely coupled, and the time constants are mixed. It is therefore rather tricky to determine the time constants by time transient decay experiments. A full spectroscopy, either based on the perturbation or the voltage (IS), or the light,¹⁰ should be used in such situation. By fitting the spectra to an appropriate model, as in the case of Fig. S6c, the parameters can be properly determined.

References

- (1) Bisquert, J.; Vikhrenko, V. S. "Interpretation of the time constants measured by kinetic techniques in nanostructured semiconductor electrodes and dye-sensitized solar cells." *J. Phys. Chem. B* **2004**, *108*, 2313-2322
- (2) Bisquert, J. "Beyond the quasi-static approximation: Impedance and capacitance of an exponential distribution of traps". *Phys. Rev. B* **2008**, *77*, 235203
- (3) Bisquert, J.; Fabregat-Santiago, F.; Mora-Seró, I.; Garcia-Belmonte, G.; Giménez, S. "Electron Lifetime in Dye-Sensitized Solar Cells: Theory and Interpretation

of Measurements". *J. Phys. Chem. C* **2009**, *113*, 17278–17290

(4) Cao, Y.; Bai, Y.; Yu, Q.; Cheng, Y.; Liu, S.; Shui, D.; Gao, F.; Wang, P. "Dye-Sensitized Solar Cells with a High Absorptivity Ruthenium Sensitizer Featuring a 2-(Hexylthio)thiophene Conjugated Bipyridine". *J. Phys. Chem. C* **2009**, *113*, 6290–6297

(5) Sze, S. M. *Physics of Semiconductor Devices*, 2nd ed.; John Wiley and Sons: New York, 1981.

(6) Södergren, S.; Hagfeldt, A.; Olsson, J.; Lindquist, S. E. "Theoretical Models for the Action Spectrum and the Current-Voltage Characteristics of Microporous Semiconductor Films in Photoelectrochemical Cells". *J. Phys. Chem.* **1994**, *98*, 5552-5556

(7) Bisquert, J. "Theory of the Impedance of Electron Diffusion and Recombination in a Thin Layer". *J. Phys. Chem. B* **2002**, *106*, 325-333

(8) Wang, Q.; Ito, S.; Grätzel, M.; Fabregat-Santiago, F.; Mora-Seró, I.; Bisquert, J.; Bessho, T.; Imai, H. "Characteristics of High Efficiency Dye-sensitized Solar Cells". *J. Phys. Chem. B* **2006**, *110*, 19406-19411

(9) Pitarch, A.; Garcia-Belmonte, G.; Mora-Seró, I.; Bisquert, J. "Electrochemical impedance spectra for the complete equivalent circuit of diffusion and reaction under steady-state recombination current". *Phys. Chem. Chem. Phys.* **2004**, *6*, 2983-2988

(10) Dloczik, L.; Ieperuma, O.; Lauerma, I.; Peter, L. M.; Ponomarev, E. A.; Redmond, G.; Shaw, N. J.; Uhlendorf, I. "Dynamic Response of Dye-Sensitized Nanocrystalline Solar Cells: Characterization by Intensity-Modulated Photocurrent Spectroscopy". *J. Phys. Chem. B* **1997**, *101*, 10281-10289